



HAL
open science

Can magnetisation transfer magnetic resonance imaging help for the follow-up of synthetic hernia composite meshes fate? A pilot study

Florence Franconi, Olivier Lefranc, Amandine Radlovic, Laurent Lemaire

► To cite this version:

Florence Franconi, Olivier Lefranc, Amandine Radlovic, Laurent Lemaire. Can magnetisation transfer magnetic resonance imaging help for the follow-up of synthetic hernia composite meshes fate? A pilot study. *Magnetic Resonance Materials in Physics, Biology and Medicine*, 2022, 10.1007/s10334-022-01016-4 . hal-03669287

HAL Id: hal-03669287

<https://univ-angers.hal.science/hal-03669287>

Submitted on 16 May 2022

HAL is a multi-disciplinary open access archive for the deposit and dissemination of scientific research documents, whether they are published or not. The documents may come from teaching and research institutions in France or abroad, or from public or private research centers.

L'archive ouverte pluridisciplinaire **HAL**, est destinée au dépôt et à la diffusion de documents scientifiques de niveau recherche, publiés ou non, émanant des établissements d'enseignement et de recherche français ou étrangers, des laboratoires publics ou privés.

Can magnetisation transfer Magnetic Resonance Imaging help for the follow-up of synthetic hernia composite meshes fate? A pilot study

Franconi Florence^{1,2}, Olivier Lefranc³, Amandine Radlovic³, Laurent Lemaire^{1,2}

Franconi Florence: ORCID 0000-0001-6725-0803 ; Lemaire Laurent : ORCID 0000-0002-1308-9345

¹UNIV ANGERS, PRISM – Plateforme de Recherche en Imagerie et Spectroscopie Multimodales, 4 rue Larrey, Angers 49933, France

²UNIV ANGERS, INSERM UMR-S 1066- CNRS 6021, Micro et Nanomédecines Translationnelles – MINT Université d'Angers, 4 rue Larrey, Angers 49933, France

³SOFRADIM Production, 116 avenue du Formans, 01600 Trevoux, France.

Correspondence to: laurent.lemaire@univ-angers.fr

Abstract :

Purpose:

This study aims at evaluating the non-invasive Magnetic Resonance Imaging (MRI) technic to visualize a synthetic composite hernia mesh using a rodent model and to document the integration of this device over 4 months.

Methods:

Uncoated polyethylene terephthalate mesh and synthetic composite mesh—faced on the visceral side with a chemically engineered layer of copolymer of glycolide, caprolactone, trimethylene carbonate, and lactide to minimize tissue attachment—were placed intraperitoneally in rats, facing the caecum previously scraped to promote petechial bleeding and subsequent adhesions. Meshes fate follow-up was performed 4, 10, and 16-weeks post-implantation using a rodent dedicated high field MRI. Magnetization transfer (MT) images were acquired, associated with pneumoperitonealMRI performed after intraperitoneal injection of 8 mL gas to induce mechanical stress on the abdominal wall.

Results:

Uncoated meshes were clearly visible using both T2-weighted and MT imaging during the whole study while composite meshes conspicuity was not so evident on T2-weighted MRI and could be improved using MT imaging. Adhesions and collagen infiltration were massive for the uncoated meshes as expected. On the contrary, composite meshes showed very limited adhesion, and, if any, occurring at the edge of the mesh, starting at the fixation points.

Conclusions:

Magnetization transfer imaging allows to detect mesh integration and, associated with pneumoperitoneum, was able to probe the effective minimizing effect of the synthetic polymeric barrier on visceral attachments. However, magnetization transfer imaging could not unambiguously allow the visualization of the mesh through the polymeric barrier.

Ventral hernia repair - MRI - Magnetization transfer - Pneumoperitoneum - Mesh - Visceral attachment

Published in Magn Reson Mater Phys, 2022, DOI 10.1007/s10334-022-01016-4

Introduction

Hernia textile-based meshes are intended for the reinforcement of abdominal wall soft tissue where weakness exists. Intra-abdominal meshes are frequently used for ventral hernia repair (VHR) and are associated with a low hernia recurrence rate when compared to simple surgical suturing of the abdominal wall hernia defects[1]. Intra-abdominal hernia mesh key characteristics include excellent biocompatibility so it integrates well into the abdominal wall tissue, and low to lack of

adhesiogenicity minimizes abdominal adhesion to the mesh [1]. One strategy to decrease the adhesiogenicity of textile-based intra-abdominal meshes is to coat one of the surfaces of the mesh with a minimizing tissue attachment barrier that decreases the risk of abdominal adhesion to form. This type of mesh is called composite mesh. Despite the usage of composite meshes with optimal characteristics post-operative complications may still occur due to both the direct contact between the mesh and the abdominal viscera and the

inflammatory reaction that occur as a consequence of the implantation of the mesh in living tissue and of the resulting wound healing process. One of the leading complications associated with the use of intra-abdominal meshes is the development of abdominal adhesions[2]. There is therefore a critical need for non-invasive medical imaging tools and techniques to assess and document post-implantation mesh evolution and to better diagnose complications such as intra-abdominal adhesion. Computed tomography and ultrasonography are the commonly used non-invasive medical imaging technique used to clinically postoperatively monitor VHR patients [3]. These methods remain with limited performances when it comes to detect thin polymeric materials and abdominal visceral adhesions. Mesh visualization using Magnetic Resonance Imaging (MRI) technique has been achieved after contrast agent incorporation into meshes to make them MRI-visible[4–9]. A recent preclinical study showed that a collagen coated mesh can be imaged over time using Amide Proton transfer MRI[10]. Regarding abdominal adhesions to the mesh, Cine-MRI in humans[11] and in experimental rodents using pneumoperitoneal-MRI[12] was proven useful to document this side effect. Despite the large range of offered contrasts, the high spatial resolution and the absence of radiation exposure, MRI usually does not allow to easily image the meshes and remains an emerging technique for the exploration of VHR complications.

The aim of this study was therefore to evaluate the integration and the minimization of visceral attachments of an intra-abdominal synthetic hernia mesh, using long-term non-invasive MRI longitudinal follow-up. The Behaviour of a macroporous polypropylene mesh, covered on one side with a barrier layer of copolymer of glycolide, caprolactone, trimethylene carbonate, and lactide, was explored in a rodent caecal abrasion model[12, 13] and compared to the fate of a bare polyethylene terephthalate hernia mesh.

Materials and methods:

In vivo mesh implantation

The study was performed following the regulations of the French Ministry of Agriculture and the protocol was approved by the Committee for the Ethics of Animal Experiments of the 'Pays de la Loire' (Permit no. APAFIS#1733-2015083114252179) in accordance with the EU Directive 2010/63/EU.

Two types of meshes were used in this study. Each type of mesh was implanted in Sprague-Dawley rats (240-320g, Angers University/Hospital animal

Facility, Angers, France) (n=6 per type of mesh). The first type of mesh was a synthetic composite mesh composed of a non-resorbable macroporous polypropylene textile coated on one side with an absorbable synthetic resorbable barrier (copolymer glycolic acid/lactic acid/trimethylene carbonate/caprolactone) for minimizing tissue attachment to the mesh [14]. The second type of mesh was a polyethylene terephthalate (PET) multifilament textile without barrier. The PET was used as a positive control for the development of soft tissue visceral attachment [12, 15] to the mesh. Tissue attachments was induced, using a caecal abrasion and a peritoneal defect model previously described [12, 13]. Briefly, fifteen minutes before the surgery, rats were injected intramuscularly with 10µg/kg Buprenorphine (Vetergesic, Sogeval, France) for perioperative pain relief. Under isoflurane anaesthesia (Isoflurane Belamont, France, 5-2%, O₂: 0.8L/min) a midline incision of the skin and abdominal wall, the caecum was externalized and abraded using gauzes and a scalpel. The caecum was then allowed to air dry and during this period, a surgical defect was created by removing the peritoneum and some muscle fibers of the abdominal wall facing the cecum. The tested meshes (25mm X 15mm) were sutured to the abdominal wall over the peritoneal defect with a non-absorbable 6/0 suture with one stitch at each corner of the article. The composite mesh was placed with the minimizing tissue attachment barrier facing the abraded cecum. The linea alba was sutured with a non-absorbable suture and the cutaneous layer was closed using a running stitch of an absorbable suture. A dressing was applied to the abdomen. The rats were allowed to recover in individual cages for 24h, before being housed in pair to respect their social behaviour.

In vivo Magnetic Resonance Imaging.

MRI examination of the abdominal cavity was performed with a 7T scanner (Biospec 70/20 Avance III, Bruker, Wissembourg, France) equipped with a BGA12S gradient system (675mT/m) and a 72-mm proton volume resonator for radiofrequency excitation and signal reception. All imaging acquisitions were performed using ParaVision ® 6.0.1, under isoflurane anesthesia (5-2%, O₂: 0.8L/min). Animal body temperature was maintained throughout the experiment by hot water circulation in the animal bed. Respiration was monitored using a small animal monitoring and gating system, model 1025, SA instrument, NY, USA.

MRI visualization of the mesh was performed at 4, 10 and 16 weeks after implantation. The latest time point was chosen according to preliminary studies

that have shown that the polymeric synthetic barrier resorbs within 16 weeks post-implantation[14]. The 10-week time point was supposed to offer an intermediate situation whereas at 4-weeks, the polymeric film should still be in place and the remodelling/inflammation associated the mesh integration should not jeopardize the image quality. For the follow-up, all animals were scanned at weeks 4 and 10. At week-10, three animals of each group (composite mesh or PET implanted groups) were also scanned by pneumoperitoneal-MRI to visualize possible tissue adhesions before being euthanized for autopsy. The remaining 6 animals (composite mesh n=3 and PET n=3) were imaged 16 weeks after implantation to explore mesh visualization and possible visceral attachments before being euthanized for autopsy.

Mesh visualization and pneumoperitoneal-MRI by T2 weighted (T2-W)

After a set of scout images, respiration gated T2 weighted fast spin-echo images (TE/TR = 23/920ms, echo train length= 8, slice thickness = 1 mm, field of view of 55mm, matrix 256², in plane-resolution = 0.215 mm, 8 averages; with an active fat saturation using a frequency selective 90° pulse, Gaussian, 2.61ms, BW 1050 Hz, applied to a frequency offset of 3.5ppm relative to water, with gradient spoiler to suppress transverse magnetization produced by the pulse) with up to 12 slices were acquired for mesh visualization in the axial plane.

This same sequence was also used to visualize tissue adhesions by pneumoperitoneal-MRI. In this case, an abdominal wall displacement was induced before images acquisition. A 5-mm skin incision was performed, under isoflurane anaesthesia, on the right side of the rat abdomen. A 2-mm outer diameter trocar was used to pass through the muscular layer, allowing the introduction of a 1-mm diameter polypropylene catheter, which was then used for the injection of 8 mL of 0.22µm filtered air within the rat abdomen to induce abdominal distension[12].

Mesh visualization by Magnetization Transfer (MT) MRI

Magnetization transfer images were obtained with a gradient echo FLASH sequence (TE/TR = 2.4/33ms, flip angle 10°, one slice of 1mm thickness, field of view of 55mm, matrix 139x172 reconstructed to 256², in plane-resolution = 0.215 mm, 40 averages and fat saturation active) with or without saturation. The saturation was obtained using a Gaussian radiofrequency pulse of 20ms with a peak B1 amplitude of 25µT at an offset frequency of 2000Hz. Magnetization transfer ratio (MTR) was

measured on MTR calculated images according to the following formula $100 \cdot (M_{\text{Toff}} - M_{\text{Ton}}) / M_{\text{Toff}}$. MTR at the mesh level was measured from regions of interest drawn on the T2 anatomical images, pasted on the MTR images after thresholding. Thresholding was performed by eliminating the populations of low or high MTR pixels whose occurrence was less than 20% of the population of the most represented pixels. This thresholding allowed to remove obviously inaccurately calculated MTR leading to a reduction of the surface area of about 20%.

Histological analysis

At 16-week time point, macroscopical observations of the meshes were performed before careful harvesting and fixation in formalin solution for further histological preparation and analysis.

For slide preparation, the samples were dried, dehydrated, and embedded in paraffin. Transversal microtome cutting (4µm slide thickness), on the medial and distal areas of the samples was performed. For each slide, 2 samples were prepared and stained by Haematoxylin-Eosin (HE) and Masson Trichrome (TM).

The slides were then scanned using an Aperio Scanscope CS2, Leica. Collagen content surrounding the meshes were evaluated using ImageJ. Cellular identification was performed according to cell morphology.

Statistics

This study is mainly descriptive. No statistics are carried out on the MTR data points as they are numerously too limited. The statistical power associated with the different tests is too low in this context to consider implementing them in a relevant and adequate way.

Results:

After 4 weeks, bare PET meshes were clearly visible during MRI examination on all rats, appearing as a heterogeneous line on T2 weighted images, up to 1.5mm thick, (figures 1 a and 2 a). For all the animals, the mesh was located right over the cecum. The PET mesh contrast on the T2 weighted images stayed stable for the 16 weeks study period in all the animals (figure 2 a, e, i). PET meshes were clearly visible on MTR images throughout the entire experimental procedure (figure 2 b, f & j). The mean MTR for the PET mesh (n=6) is 75±7 at 4 weeks, 75±4 at 10 weeks & 74±1 at 16 weeks (figure 3). The synthetic composite meshes detection was not

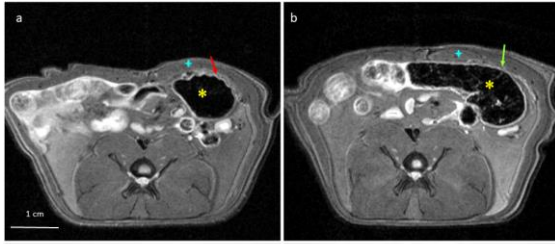


Figure 1 : Meshes implantation: meshes were fixated by four stitches to the abdominal wall (blue mark) facing the caecum (yellow mark). Axial T2-weighted images show the meshes localisation 4 weeks after implantation of PET (a) pointed by a red arrow and of composite mesh (b) by a green one.

evident on T2-weighted images. The meshes appeared as a thin line of up to 0.5mm of thickness (figures 1 b and 2 c). Ten and sixteen weeks after implantation, the visualization remained not obvious (figure 2 g, k).

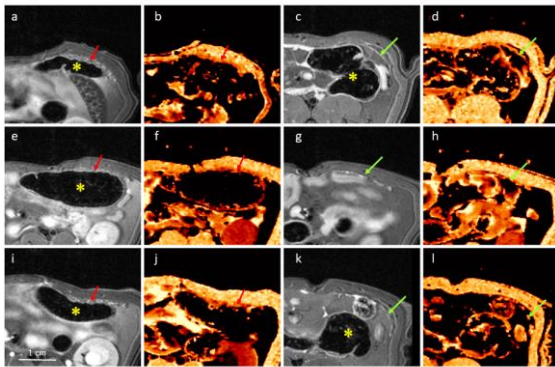


Figure 2: Representative axial magnetization transfer (b, d, f, h, j, l) and corresponding T2-weighted images (a, c, e, g, i, k) of PET (pointed by a red arrow) and composite mesh (pointed by a green arrow) meshes at 4 (a-d), 10 (e-h) and 16 (i-l) weeks after implantation. The caecum is pointed by the yellow mark.

For better contrast, magnetization transfer images were acquired. Four weeks after implantation, the composite meshes appear as a thin line with an MTR ratio of 75 ± 3 whereas the abdominal wall was characterized by an MTR ratio of 83 ± 4 (figure 3).

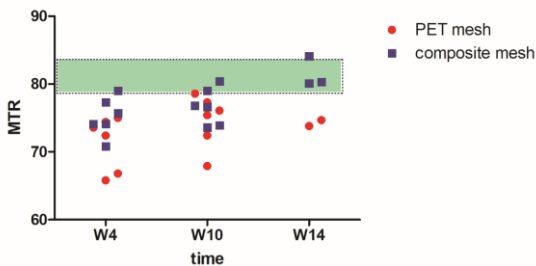


Figure 3: Evaluation of MTR evolution with mesh integration. Red circles (O) correspond to MTR values measured for the bare 3D PET mesh and blue squares (●) to values measured for the composite mesh. The dashed box corresponds to the the normal values in abdominal wall.

At later experimental points, the MTR ratio at the mesh level was equivalent to the MTR ratio within the abdominal wall (figure 3) suggesting an efficient integration of the mesh without massive remodeling (figure 2 h, l). This observation has to be considered in the light of the histological analysis showing the thin layer of collagen surrounding the composite meshes as opposed to the substantial collagen deposit onto the thicker PET mesh (figure 4A). A detailed analysis of the histological slices 16 weeks post-implantation reveals that in the composite mesh vicinity (figure 4B, collagen production is limited and represents, in surface, 25-30% of the implant. Giant cells, illustrating the reaction to foreign body are numerous limited (figure 4D). Regarding the bare PET mesh, the collagen deposit is more important as it represents 40-50% of the implant surface. Giant cells are also limited in numbers (figure 4C).

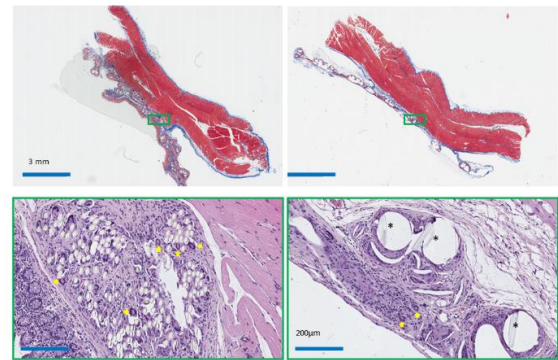


Figure 4 : Representative histological slice of bare 3D PET (frames A-C) and composite (frames B-D) meshes 16 weeks post implantation. Frames A & B are Masson trichrome staining and frames C & D are enlargement of H&E staining. Yellow arrows point at giant cells and stars at yarns.

Alongside with mesh detection, visceral attachments to the meshes at 10 weeks and 16 weeks post-implantation, using pneumoperitoneal-MRI before necropsy was assessed. This technique consists in the injection of gas within the abdomen of the rats in order to displace the abdominal wall at distance from the visceral tissue. As the meshes are attached to the abdominal wall when implanted, if subsequent adherences occur, any displacement of the wall will pull the visceral tissue and reveal the attachment. Ten weeks (figure 5a) or 16 weeks after implantation (figure 5c), massive adhesions are observed between the bare PET meshes and the caecum, the latest remaining in contact with the mesh despite the gas injection. This close contact was confirmed at necropsy (figure 6), as expected for a positive control. On the contrary, none of rats implanted with the synthetic composite meshes presented massive caecal adhesion or visceral attachment, the injected air being freely distributed between the guts and the

mesh. Only focal adhesions at fixation point (suture) or to conjunctive tissue (figures 5b and 6b) were observed.

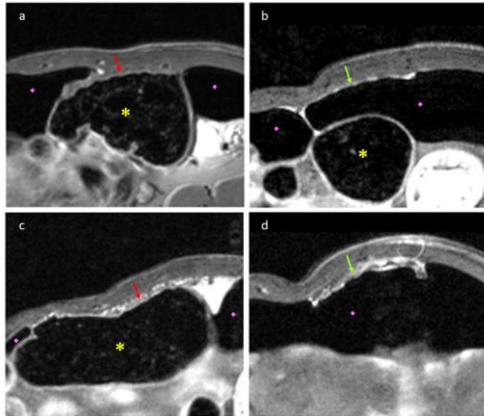


Figure 5 : Representative pneumoperitoneal-MRI of PET (a, c), pointed by a red arrow, and composite mesh (b, d), pointed by a green arrow, acquired 10 (a-b) and 16 (c-d) weeks after implantation are presented. The caecum is pointed by the yellow mark and the injected air by the pink one.

Discussion:

MRI is not the common method in clinical practice to monitor mesh outcome even though this method is reported in some preclinical or clinical researches[10, 12, 16, 17] and present the major advantage to provide the ability for long term follow up of the same individual in a non-invasive manner. The major limitation of MRI to image intra-abdominal meshes is linked to the thinness of the polymeric mesh filaments and their short signal relaxation times T2 that make them appear usually as dark fine lines or spots on the T2-weighted MR images. This characteristic was even reinforced with the association of iron oxide nanoparticles within the filament [17–19]. However, this type of contrast enhancement can also be jeopardized by the normal post-surgical evolutions or complications such as seroma, local inflammation, or foreign body reaction[3]. Besides, the abdominal environment is complex, with peristaltic or respiratory displacement that can impair the image quality when long acquisition time is required, even though the latter can be easily compensated with a respiration-triggered acquisition. So, depending on the adjacent structures signal (moderate intensity for abdominal wall or fat, no signal in the caecum), the mesh can be difficult to distinguish from the background.

The emergence of barrier coated meshes, covered on one face with biological material such as hyaluronic acid/carboxymethyl cellulose (Sepramesh™) or collagen (Parietex™) to minimize visceral attachments once implanted into the peritoneal cavity could also be of interest from an MRI detectability point of view. Indeed for collagen

coated, the presence of amide function can be used to create a contrast using amide proton transfer[10]. Nowadays, attention is also given to fully synthetic meshes with chemically engineered coating to minimize attachment. In the present study, we are exploring the MRI ability to document the fate of a synthetic composite mesh after implantation in a Rodeheaver type hernia model [12, 13] as compared to a non-coated non-resorbable polyethylene terephthalate (PET) mesh used as a positive control for tissue attachment[12]. The studied composite mesh composed was made of non-absorbable polypropylene monofilament knitted textile, to favor tissue integration, and faced on one side with the absorbable synthetic copolymer of glycolide, caprolactone, trimethylene carbonate and lactide to minimize tissue attachment was proposed. As the polymeric synthetic barrier is to be resorbed within 105 days[14], the follow up was planned for 4 months. In all animals enrolled in the present study and at each time points, whatever the mesh type, the prostheses were localised using standard T2-weighted MRI (figure 2). The wider appearance of the thicker PET mesh compared to the composite mesh was mainly due to a higher deposit of collagen (figure 4). As expected, PET meshes bearing rats' present massive attachment of the caecum membrane in contact with the mesh, as suggested by the 'wavy shape' and confirm on pneumoperitoneum MRI (Figure5) or at necropsy (figure6). This phenomenon was observed in all six rats. It should be noted that the localisation by the massive rat caecum, appearing as a hyposignal, greatly facilitate the mesh delineation. On the contrary, for the composite mesh the depiction can only be gained due to the high image resolution that can be achieved with the dedicated rodents MRI (figure 2). Moreover, the presence of the adherence limiting coating led to minimal adhesions between the caecum and the mesh as seen on the pneumoperitoneum MRI (figure 5) and at necropsy (figure 6), which does not allow to benefit from intrinsic contrast brought by the caecum.

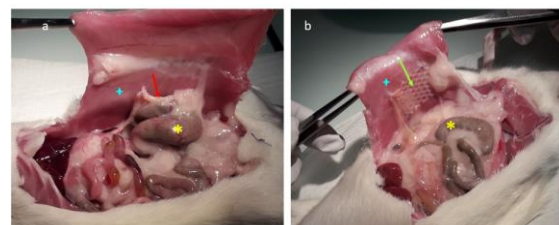


Figure 6 : Representative necropsy of PET (a), pointed by a red arrow, and composite mesh (b), pointed by a green arrow, meshes 16 weeks after implantation. The caecum is pointed by the yellow mark and the abdominal wall by the blue one.

The originality of this work stands on the evaluation of magnetization transfer MRI (MT-MRI) to depict mesh through the adherence limiting polymeric face and characterize the integration and remodelling associated with the implantation. MT-MRI is based on the magnetization exchange between two proton pools, the macromolecular bound water protons and the unbound water ones [20, 21]. We have hypothesized that the presence of the polymeric resorbable barrier should be hydrated and therefore could constitute the bound water protons pool and could therefore allow the visualization of this barrier, at least at the early time point. However, and as shown in **figure 3** The MTR measured at the coated or uncoated mesh level 4 and 10 weeks post-implantation are similar and reduced compared to normal muscle, suggesting that the contrast is more driven by the inflammation induced by the implantation rather than to the polymeric film. The persistence of the composite mesh contrast observed on the MT images at 16 weeks is not consistent with mesh lifespan as it has been established that the barrier is resorbed within 105 days[14] and the change may reflect the natural evolution from an inflammatory situation to an integrative situation with deposit of a thin layer of neo-collagen [22] as observed on the trichrome staining. Consequently, depiction of the adhesion limiting polymeric mesh layer could not be achieved using MT imaging. Nevertheless, and according to the MTR evolution with time, MT imaging might be a useful tool to evaluate the integration of the mesh and collagen deposit associated with the implant. The normalization of the MTR at the composite mesh level reflecting the efficient integration whereas the remaining low MTR value at the control bare-PET mesh reflecting the thick collagen deposit within the multifilament's structure.

CONCLUSION:

A durable ventral hernia repair success is based on a good abdominal wall integration linked to fibrin deposition on mesh knitted pattern induced by a moderate inflammatory response and fibroblast influx. However, this inflammatory response has the potential to induce large abdominal adhesions and be source of pain. The barrier layer of the composite mesh is there to minimize the tissue attachment to the meshes. Non-invasive follow up of meshes to document mesh tissue integration remains a challenge, especially for meshes without contrast agent incorporation. Magnetization transfer magnetic resonance imaging, a technique based on the dynamic exchange of water molecules between hydrated macromolecules and the pool of unbounded water molecules appears as a promising

technique as shown in the present pre-clinical study and, associated with pneumoperitoneal-MRI, allows the unambiguous evaluation of the barrier effect on tissue adhesion, allows the evaluation of the integration, but does not unambiguously allow the depiction of the mesh through the thin synthetic layer.

Conflict of interest disclosure:

O. Lefranc and A. Radlovic are Medtronic employees. L. Lemaire and F. Franconi have no conflicts to disclose.

Authors' contribution:

The authors confirm contribution to the paper as follows: Study design and conception: O. Lefranc, L. Lemaire, F. Franconi & A. Radlovic; data collection, interpretation and Analysis: F. Franconi & L. Lemaire; Draft manuscript preparation: F. Franconi. All authors reviewed the results and approved the final version.

BIBLIOGRAPHY:

1. Cevasco M, Itani KMF (2012) Ventral Hernia Repair with Synthetic, Composite, and Biologic Mesh: Characteristics, Indications, and Infection Profile. *Surgical Infections* 13:209–215. <https://doi.org/10.1089/sur.2012.123>
2. Lefranc O, Bayon Y, Montanari S, Gravagna P, Thérin M (2011) Reinforcement Materials in Soft Tissue Repair: Key Parameters Controlling Tolerance and Performance – Current and Future Trends in Mesh Development. In: von Theobald P, Zimmerman CW, Davila GW (eds) *New Techniques in Genital Prolapse Surgery*. Springer London, London, pp 275–287
3. Patil AR, Nandikoor S, Mohanty HS, Godhi S, Bhat R (2019) Mind the gap: imaging spectrum of abdominal ventral hernia repair complications. *Insights into Imaging* 10. <https://doi.org/10.1186/s13244-019-0730-x>
4. Ciritsis A, Hansen NL, Barabasch A, Kuehnert N, Otto J, Conze J, Klinge U, Kuhl CK, Kraemer NA (2014) Time-Dependent Changes of Magnetic Resonance Imaging-Visible Mesh Implants in Patients: *Investigative Radiology* 49:439–444. <https://doi.org/10.1097/RLI.0000000000000051>
5. Guillaume O, Blanquer S, Letouzey V, Cornille A, Huberlant S, Lemaire L, Franconi F, Tayrac R de, Coudane J, Garric X (2012) Permanent Polymer Coating for in vivo MRI Visualization of Tissue Reinforcement Prostheses.

- Macromolecular Bioscience 12:1364–1374. <https://doi.org/10.1002/mabi.201200208>
6. Blanquer S, Guillaume O, Letouzey V, Lemaire L, Franconi F, Paniagua C, Coudane J, Garric X (2012) New magnetic-resonance-imaging-visible poly(epsilon-caprolactone)-based polyester for biomedical applications. *Acta Biomaterialia* 8:1339–1347. <https://doi.org/10.1016/j.actbio.2011.11.009>
 7. Krämer NA, Donker HCW, Otto J, Hodenius M, Sénégas J, Slabu I, Klinge U, Baumann M, Müllen A, Obolenski B, Günther RW, Krombach GA (2010) A Concept for Magnetic Resonance Visualization of Surgical Textile Implants: *Investigative Radiology* 45:477–483. <https://doi.org/10.1097/RLI.0b013e3181e53e38>
 8. Letouzey V, Huberlant S, Cornille A, Blanquer S, Guillaume O, Lemaire L, Garric X, de Tayrac R (2015) Tolerance and Long-Term MRI Imaging of Gadolinium-Modified Meshes Used in Soft Organ Repair. *PLOS ONE* 10:e0120218. <https://doi.org/10.1371/journal.pone.0120218>
 9. Schulz A, Lemaire L, Bethry A, Allègre L, Cardoso M, Bernex F, Franconi F, Goze-Bac C, Taillades H, Garric X, Nottelet B (2019) UV-triggered photoinjection of contrast agent onto polymer surfaces for *in vivo* MRI-visible medical devices. *Multifunctional Materials* 2:024001. <https://doi.org/10.1088/2399-7532/ab0f81>
 10. Franconi F, Roux J, Garric X, Lemaire L (2014) Early postsurgical visualization of composite mesh used in ventral hernia repair by amide proton transfer MRI. *Magn Reson Med* 71:313–7. <https://doi.org/10.1002/mrm.24666>
 11. Langbach O, Holmedal SH, Grandal OJ, Røkke O (2016) Adhesions to Mesh after Ventral Hernia Mesh Repair Are Detected by MRI but Are Not a Cause of Long Term Chronic Abdominal Pain. *Gastroenterology Research and Practice* 2016:1–7. <https://doi.org/10.1155/2016/2631598>
 12. Franconi F, Roux J, Lefebvre-Lacoeuille C, Lemaire L (2014) Imaging visceral adhesion to polymeric mesh using pneumoperitoneal-MRI in an experimental rat model. *Surgical Endoscopy* 29:1567–73. <https://doi.org/10.1007/s00464-014-3843-9>
 13. Harris ES, Morgan RF, Rodeheaver GT (1995) Analysis of the kinetics of peritoneal adhesion formation in the rat and evaluation of potential antiadhesive agents. *Surgery* 117:663–669
 14. Medtronic (2019) Parietene DS Composite (TM) mesh. <http://www.tamethepain.com/content/dam/covidien/library/emea/en/product/hernia-repair/weu-parietene-ds-synthetic-barrier-brochure.pdf>
 15. Liu H, van Steensel S, Gielen M, Vercoulen T, Melenhorst J, Winkens B, Bouvy ND (2020) Comparison of coated meshes for intraperitoneal placement in animal studies: a systematic review and meta-analysis. *Hernia* 24:1253–1261. <https://doi.org/10.1007/s10029-019-02071-y>
 16. Lambertz A, van den Hil LCL, Ciritsis A, Eickhoff R, Kraemer NA, Bouvy ND, Müllen A, Klinge U, Neumann UP, Klink CD (2018) MRI Evaluation of an Elastic TPU Mesh under Pneumoperitoneum in IPOM Position in a Porcine Model. *Journal of Investigative Surgery* 31:185–191. <https://doi.org/10.1080/08941939.2017.1301599>
 17. Weyhe D, Klinge U, Uslar VN, Tabriz N, Kluge A (2019) Follow Up Data of MRI-Visible Synthetic Meshes for Reinforcement in Large Hiatal Hernia in Comparison to None-Mesh Repair—A Prospective Cohort Study. *Frontiers in Surgery* 6:. <https://doi.org/10.3389/fsurg.2019.00017>
 18. Awada H, Al Samad A, Laurencin D, Gilbert R, Dumail X, El Jundi A, Bethry A, Pomrenke R, Johnson C, Lemaire L, Franconi F, Félix G, Larionova J, Guari Y, Nottelet B (2019) Controlled Anchoring of Iron Oxide Nanoparticles on Polymeric Nanofibers: Easy Access to Core@Shell Organic–Inorganic Nanocomposites for Magneto-Scaffolds. *ACS Applied Materials & Interfaces* 11:9519–9529. <https://doi.org/10.1021/acsami.8b19099>
 19. Sindhwani N, Callewaert G, Deprest T, Housmans S, Van Beckevoort D, Deprest J (2018) Short term post-operative morphing of sacrocolpopexy mesh measured by magnetic resonance imaging. *Journal of the Mechanical Behavior of Biomedical Materials* 80:269–276. <https://doi.org/10.1016/j.jmbbm.2018.02.012>
 20. Chen B, Zhao Y, Cheng X, Ma Y, Chang EY, Kavanaugh A, Liu S, Du J (2018) Three-dimensional ultrashort echo time cones (3D UTE-Cones) magnetic resonance imaging of entheses and tendons. *Magnetic Resonance Imaging* 49:4–9. <https://doi.org/10.1016/j.mri.2017.12.034>
 21. Henkelman RM, Stanisz GJ, Graham SJ (2001) Magnetization transfer in MRI: a review. *NMR in Biomedicine* 14:57–64. <https://doi.org/10.1002/nbm.683>
 22. Laurent D, Wasvary J, Yin J, Rudin M, Pellas TC, O’Byrne E (2001) Quantitative and qualitative assessment of articular cartilage in the goat knee with magnetization transfer imaging. *Magnetic Resonance Imaging* 19:1279–1286. [https://doi.org/10.1016/S0730-725X\(01\)00433-7](https://doi.org/10.1016/S0730-725X(01)00433-7)